Spectroscopy of ^{34,35}Si by β decay: sd-fp shell gap and single-particle states

S. Nummela,[1,2] P. Baumann,[3] E. Caurier,[3] P. Dessagne,[3] A. Jokinen,[1,2] A. Knipper,[3] G. Le Scornet,[4,5] C. Miehé,[3] F. Nowacki,[6] M. Oinonen,[5] Z. Radivojevic,[1] M. Ramdhane,[7] G. Walter,[3] J. Äystö,[1,5] and the ISOLDE Collaboration

[1]*Department of Physics, University of Jyväskylä, P.O. Box 35, Jyväskylä, Finland*

[2]*Helsinki Institute of Physics, University of Helsinki, Finland*

[3]*IReS, IN2P3-CNRS, Louis Pasteur University, Boîte Postale 28, F-67037 Strasbourg Cedex, France*

[4]*CSNSM, F-91405 Campus Orsay, France*

[5]*EP-Division, CH-1211 Geneva, CERN, Switzerland*

[6]*Theoretical Physics Laboratory, F-67084 Strasbourg Cedex, France*

[7]*University of Constantine, Constantine, Algeria*

(Received 12 May 2000; published 19 March 2001)

The ^{34,35}Al β decays have been studied at the CERN online mass separator ISOLDE by β-γ, β-γ-γ, and β-n-γ measurements in order to corroborate the low-level description of ^{34}Si and to obtain the first information on the level structure of the $N=21$ isotope ^{35}Si. Earlier observed γ lines in ^{34}Al decay were confirmed and new γ transitions following both β decay and β-delayed neutron emission have been established. The first level scheme of ^{35}Si includes three excited states at 910, 974, and 2168 keV. Indication is found for $J^{\pi}=(3/2)^{-}$ and $(3/2)^{+}$ for the first two excited states, respectively. Beta-decay half-life of $T_{1/2}=38.6(4)$ ms and β-delayed neutron branching value $P_n=41(13)\%$ were measured unambiguously. The significance of the single-particle energy determination at $N=21$, $Z=14$ for assessing the effective interaction in sd-fp shell-model calculations is discussed and illustrated by predictions for different neutron-rich isotopes.

DOI: 10.1103/PhysRevC.63.044316 PACS number(s): 23.40.Hc, 21.60.Cs, 27.30.+t, 23.20.Lv

I. INTRODUCTION

Recently, several independent measurements on the study of neutron-rich nuclei located near the $N=20$ and $N=28$ shell closures ($Z=20$) have been carried out with different approaches and techniques [1–5]. The vast interest for this region dates back to a measurement by Thibault *et al.* [6] when a region of strong deformation, unexpected by the sd-shell model, was discovered around $Z=11$, $N=20$. At the present time, more recent experimental data on masses, level structure, and transition probabilities [7–10] have incited refined theoretical calculations [11–20] for different configurations around the $N=20$ shell closure. It has already been shown through β-decay studies that ^{34}Si lies at the edge of this deformed island [21] in the (N,Z) plane, having a $0p$-$0h$ ground state, while its two lowest excited states have a large fp-shell intruder component.

Recent measurements of $B(E2)$ and the energy of 2_1^+ states performed at MSU [2] for even $^{32-38}$Si isotopes confirm and extend our previous results. By assuming an $N=20$ closed shell for $N>20$ silicon isotopes, the experimental 2_1^+ states can be reproduced. An additional source of information on the interplay between $0\hbar\omega$ and $2\hbar\omega$ states at $N=20$ would be the experimental confirmation of a 0_2^+ intruder state at low energies in ^{34}Si as predicted by different calculations [2,16,20,21]. As much interest has been devoted recently to this question, we have searched for γ transitions that could be related to such a level structure. However, the main goal of the present work was to obtain the low-energy level structure of the $N=21$ ^{35}Si isotope. As a matter of fact, in shell-model studies, the evolution of single-particle energies plays an important role in determining the effective interactions between valence particles. With the experimental data on the first excited states of ^{35}Si ($N=21$), which up to now were unknown, we can extend the test of the evolution of single-particle $p_{3/2}$ and $d_{3/2}$ states of $N=21$ isotones starting from $Z=20$ (^{41}Ca) down to $Z=14$ (^{35}Si).

Motivated by these basic questions on the shell-model predictions around $N=20$, we carried out a study of the ^{34,35}Al β decay at CERN using the ISOLDE online separator. The results will be discussed in the framework of a shell-model calculation performed in the full (sd-fp) space. Preliminary results of the present work have been reported in [22,23].

II. EXPERIMENTAL PROCEDURES

^{34,35}Al activities were produced at the ISOLDE facility at CERN in fragmentation reactions with a pulsed 1 GeV proton beam from the PS-Booster impinging on a uranium carbide target with a thickness of 46 g cm^{-2} for uranium. The intensity of the proton beam was 3×10^{13} ions/pulse, the time interval between pulses being a multiple of 1.2 s. The average beam current was above 2 μA. The reaction products were ionized in a tungsten surface-ionization source and separated by mass. With this target-ion source device, the highest yield usually corresponds to alkalis. However, in the mass range $33<A<35$, the Na isotopes give a minor contribution to the radioactive beam, the essential part of it being the directly produced Al isotopes. The yield for mass-separated ^{34}Al isotopes was 30 atoms/s while for ^{35}Al it was close to 10 atoms/s. Ions were collected onto a tape that was moved periodically in order to reduce the amount of contaminants and longer-lived daughter activities. The experimental setup, which was assembled around the collection

point, was designed to detect β particles, γ rays, and β-delayed neutrons. A thin cylindrical plastic detector, covering a large fraction of the total solid angle around the collection point, was used for triggering β-γ coincidences and provided a start signal for neutron time-of-flight measurements. Two large-volume Ge detectors recorded γ rays both as β-γ and β-γ-γ coincidences. For β-delayed neutron time-of-flight measurements, eight low-threshold neutron detectors were located around the collection point each with the same flight path of 50.8 cm. These detectors were small plastic scintillators (1 cm thick, 10 cm in diameter), each viewed by two XP2020/URQ phototubes operating in coincidence as described in Ref. [24]. Their intrinsic efficiency was about 12% and the variation of the efficiency with the neutron energy was evaluated during the same run by measuring the delayed-neutron spectrum of ^{29}Na for which the relative intensity of the neutron branches have been measured previously [25,26].

For both masses, $A=34$ and 35, two γ spectra were created during acquisition, corresponding to two consecutive time windows of the separator beam-pulsing cycle. The lengths of the time windows were adjusted according to the half-life of the first generation under study. This provided a clear identification by lifetime differences of γ rays following the β decay of ^{34}Al and ^{35}Al from those of the precursors (Na or Mg), the descendants (Si and P) and multiply charged ions (for example, ^{140}Xe, 4^+ for $A=35$). Half-lives were determined from β and γ intensities taken in 5 ms time bins during the beam-off part of the radioactive beam cycle.

The decay schemes were extended with γ-γ coincidences for the strongest γ transitions, and for some weaker transitions from singles spectra not in contradiction with the coincident spectra. Finally, some limits for level lifetimes could be determined from the β-γ coincidences measured with plastic and Ge detectors. This enabled restricting the multipolarity of the corresponding transitions and accordingly spin and parity assignments of certain levels. In the particular case of the ^{35}Si level scheme, we investigated the β-γ coincidences with improved time resolution. In a separate experiment, we employed the delayed-coincidence technique with the thin plastic scintillator and a small BaF_2 counter that has a conical shape, 2.5 and 2.0 cm diameters and 2.5 cm height, optically coupled to an XP2020/Q phototube.

III. RESULTS

A. Beta decay of ^{34}Al

By comparison with the first study of ^{34}Al [21] employing the SC beam at 600 MeV, the improvement of the production yield by a factor of 3 with the pulsed 1 GeV beam in this experiment allowed a better description of the ^{34}Al decay. The half-life is $T_{1/2}=56.3(5)$ ms, which is the weighted average of 55.6(1.3) ms from the strongest γ transitions, and 56.4(6) ms from β multiscaling. Based on ^{34}Si coincidences, the previously reported four γ transitions following the β decay of ^{34}Al were confirmed together with spin and parity assignments in the ^{34}Si level scheme [21]. Four new γ transitions were found in the γ singles spectra

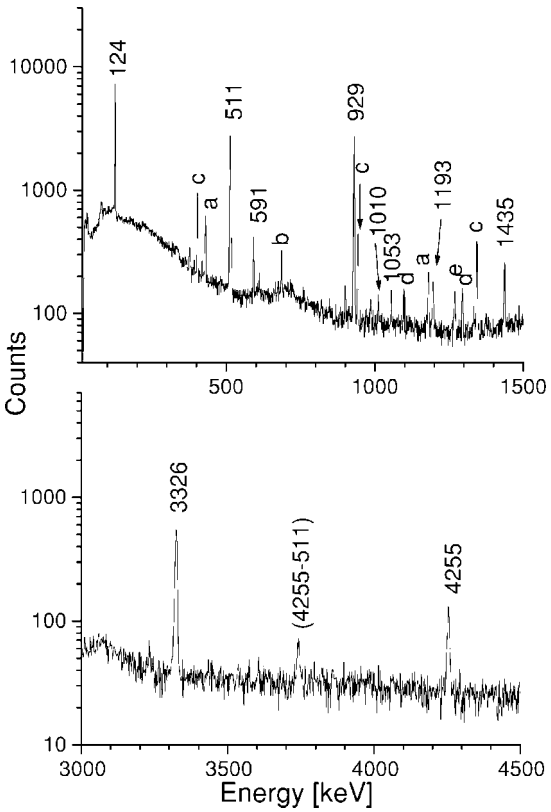

FIG. 1. Partial γ spectra taken in coincidence with β particles at $A=34$. Peaks identified by their energy in keV are from the ^{34}Al beta decay. Those labeled by a letter are from the decay of (a) ^{34}Si, (b) ^{204}At (6^+ in $A=34$), (c) ^{28}Mg, (d) ^{116}In (4^+ in $A=29$), and (e) ^{29}Al.

(Fig. 1) that can be assigned to the ^{34}Al β decay by half-life analysis. One of these transitions at 1053 keV was placed in the ^{34}Si level scheme because of the energy difference of the 4379 and 3326 keV levels. A new γ transition with an energy of 591 keV was found in coincidence with the 124 keV γ line. β-γ-γ spectra illustrating the 124, 929, and 3326 keV γ-ray sequence are shown in Fig. 2. The weaker 591 keV line is found in coincidence with the 124 keV line only due to the high detection efficiency of the 124 keV energy. We place the 591 keV transition above the 4379 keV level as no other interpretation was found. The transitions and their intensities are listed in Table I.

The 1435 keV transition can be placed in the ^{33}Si level scheme resulting from β-delayed neutron emission on the basis of two observations. First, a weak 1435 keV line was seen in coincidence with neutrons and second, this line is not observed in coincidence with high-energy betas denoting a low Q value ($S_n=7.54$ MeV in the case of ^{34}Si). An additional indication is found in the literature, as in heavy-ion induced reaction studies this energy has been attributed to a $1435\rightarrow 0$ keV transition in ^{33}Si [27,28]. In these previous works, $J^\pi=(7/2)^-$ has been proposed for the 1435 keV level. The population of a $(7/2)^-$ state in the β decay of ^{34}Al ($J^\pi=4^-$) very likely results from the deexcitation of the $(3,4)^-$ states populated by Gamow-Teller (GT) transitions

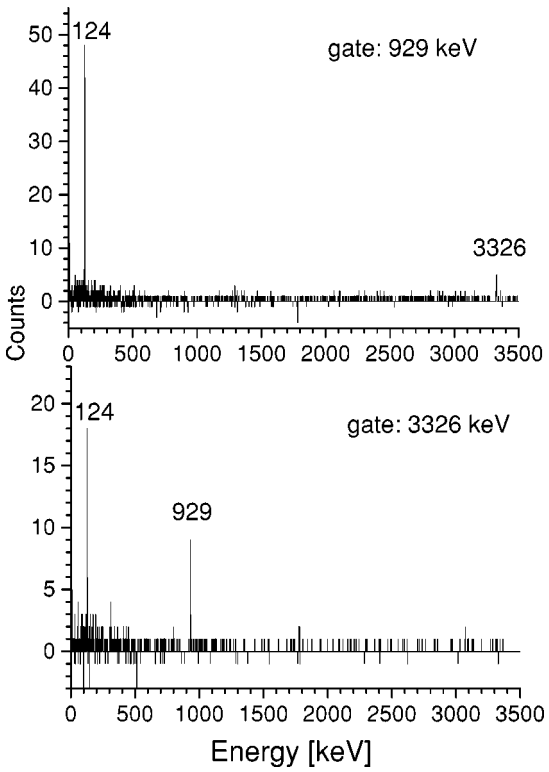

FIG. 2. β-gated γ-γ spectra at $A=34$. Coincidences with 929 keV (upper part) and 3326 keV (lower part) γ rays.

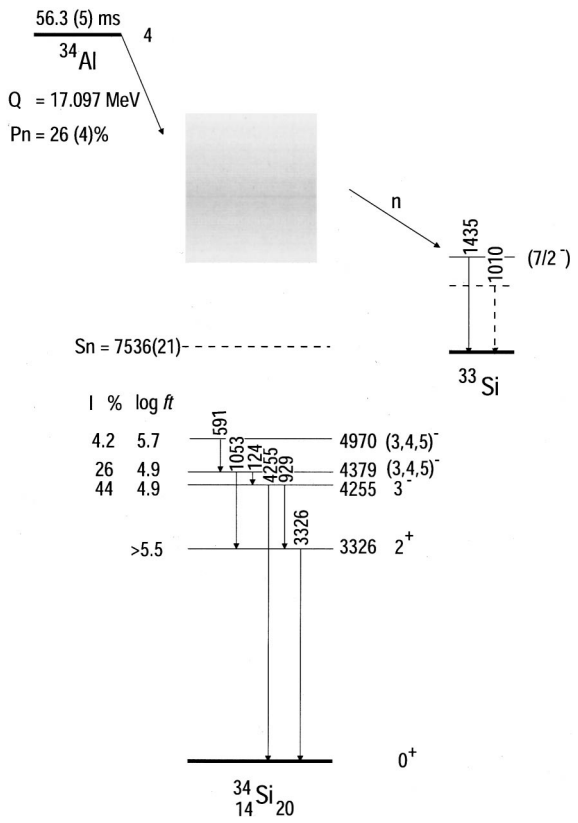

FIG. 3. ^{34}Al β-decay scheme.

through an $l=0$ neutron emission.

We observe a line at 1010 keV that was too weak to be seen in coincidence with neutrons. A state with a nearby energy has been reported in ^{33}Si by Fornal *et al.* [27] in deep-inelastic reaction studies (1010 keV) and also in heavy-ion transfer reactions by Fifield *et al.* [28] [1060(20) keV] and Mayer *et al.* [29] [1040(20) keV]. Shell-model calculations in the sd space [30] set the first excited state in ^{33}Si, $J^\pi=1/2^+$ at this energy. If the line observed in our experiment corresponds to this state, it cannot result from a direct population by β-delayed neutrons with the J^π value proposed for the ^{34}Al ground state (g.s.) ($J^\pi=4^-$). However, this state can be fed by many weak transitions in ^{33}Si from $(3/2)^+$ or $(5/2)^+$ states resulting from the deexcitation of the $(3,4)^-$ states, populated by GT transitions, through an $l=1$ neutron emission.

TABLE I. Energy and intensity of γ rays attributed to the ^{34}Al decay.

Energy (keV)	Intensity [a] (relative)	Transition from	Transition to
124.21(40)	51.9(4.3)	4379	4255
590.85(30)	7.7(0.8)	4970	4379
928.98(30)	103.9(9.7)	4255	3326
1009.69(40)	2.7(0.4)	[b]	
1052.76(40)	3.9(0.6)	4379	3326
1193.34(20)	6.4(0.8)	[c]	
1434.86(50)	13.9(1.4)	[b]	
1715.42(80)	2.4(0.4)	[d]	
2696.43(1.2)	4.8(1.0)	[d]	
3326.24(1.6)	100	3326	0
4257(3)	24.0(3.8)	4255	0

[a]Intensities are relative to the 3326 keV γ ray. The intensity per 100 β decays is obtained by multiplying by a factor of 0.55.

[b]Corresponding to transitions in the ^{33}Si level scheme following neutron emission.

[c]Unplaced, see text and the Appendix for discussion.

[d]Unplaced in the decay scheme.

In our β-γ spectrum one sees lines corresponding to the ^{33}Si β decay consecutive to the β-delayed neutron emission of ^{34}Al. Assuming the β branch from ^{33}Si [$J^\pi=(3/2)^+$] to the ^{33}P ground state [$J^\pi=(1/2)^+$] to be negligible (see Ref. [13]), we can determine the P_{1n} value from the relative intensity of the ^{33}Si and ^{34}Al filiations. This leads to a P_{1n} value of 26(4)%, which is in good agreement with the one obtained by Baumann *et al.* [27(5)%] [21] in a previous experiment using the same technique. However, the discrepancy is large compared to the value $P_n=54(12)$% reported by Bazin *et al.* [31] and by Reeder *et al.* [$P_n=12.5(25)$%] [3] using different techniques. In our data, there are no γ lines belonging to the ^{32}Si level scheme and therefore no indication for β-delayed $2n$ emission.

According to our data and using the Q_β value given in Ref. [10], a revised decay scheme of ^{34}Al is established and reported in Fig. 3. In the previous β-decay measurement of ^{34}Al [21], the first excited state at 3326 keV was assigned $J^\pi=2^+$ from the characteristics of the β and γ decay. This

TABLE II. β intensities and log *ft* values in the ^{34}Al β decay to bound levels in ^{34}Si.

E_x	I_β (%)	log *ft*	J^π
0			0^+
3326.4(3)	<12	>5.5	2^+
4255.4(5)	44(4)	4.90(6)	3^-
4379.5(5)	26(3)	4.90(5)	$(3,4,5)^-$
4970.4(7)	4.2(4)	5.70(7)	$(3,4,5)^-$

assignment has been confirmed by Coulomb excitation measurements [2]. For the 4255 keV level, $J^\pi=3^-$ are the only spin and parity values compatible with an allowed-β branch from the ^{34}Al g.s. and a strong γ transition to the ^{34}Si g.s. We note that from shell-model calculations, the g.s. of ^{34}Al could be 3^- as well as 4^- [32]. The observation of the 4255 keV transition in ^{34}Si with its lifetime properties ($\tau<1$ μs) differentiates between $E3(3^-\rightarrow0^+)$ and $M4(4^-\rightarrow0^+)$ and establishes 3^- for the 4255 keV level and therefore 4^- for the ^{34}Al g.s. For the 4379 keV state the assignment is 3^-, 4^-, or 5^- due to the allowed nature of the decay of the $J^\pi=4^-$ g.s. of ^{34}Al. The new log *ft* values and β branchings are shown in Table II. They confirm the aforementioned spin and parity assignments. Also, the new state at 4970 keV can be considered as only 3^-, 4^-, or 5^-.

As mentioned before, we have made a search of a transition to the first excited 0^+ state (0_2^+). This level is predicted below the first 2^+ state (2_1^+) in the most recent calculations [2,16,18,20], and in this experiment we foresee no direct β feeding to the 0_2^+ level but only a γ population from the 2_1^+ level. The $2_1^+\rightarrow0_2^+$ branching is expected to be only a few percent as the competing $2_1^+\rightarrow0_1^+$ transition is favored by energy. In the γ spectra gated by transitions leading to the 2_1^+ level, we did not reach an adequate level of sensitivity and no candidates could be found in the spectra with our statistics. Therefore, in order to locate the $2_1^+\rightarrow0_2^+$ transition we can only consider the lines in the β-gated γ spectra decaying with a rate compatible with the ^{34}Al half-life. This approach results in two candidates: 1193 and 1715 keV. These lines would correspond, respectively, to transitions from the 2_1^+ level to levels at 2133 or 1611 keV.

B. Beta decay of ^{35}Al

So far no indications were available on the β-decay branches of ^{35}Al. The half-life has been reported as 150(50) ms [34] and later as 30(4) ms [3] but no γ transitions have been observed. In the present experiment, the half-life could be measured from the β-counting rate as well as from the decay of the strongest γ transitions, as represented in Fig. 4. Taking the average of three independent β and one γ measurements, we obtain a weighted mean (and adopted) value of 38.6(4) ms.

The two strongest lines, with energies of 64 and 910 keV, were clearly detected in coincidence as can be seen in Fig. 5, where their coincidence spectra and the evolution of these

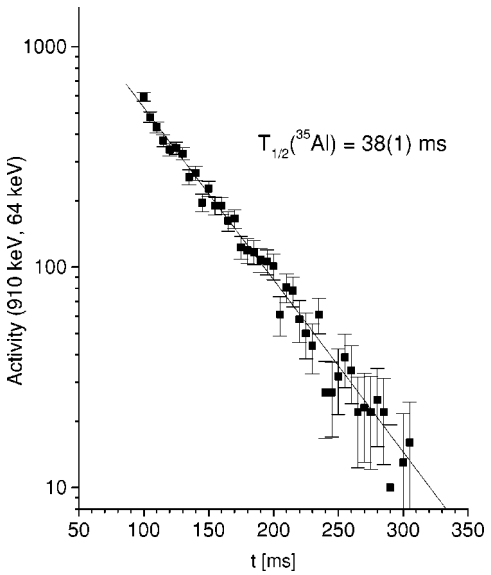

FIG. 4. Decay-time spectrum of the 64 and 910 keV lines. The result of the fit, which is indicated, has been combined with independent β measurements to get the adopted value of ^{35}Al half-life: $T_{1/2}=38.6(4)$ ms.

lines in two time bins are presented. In addition, three more transitions were observed in the β-gated γ-ray spectra and could be assigned to ^{35}Al decay on the basis of their decay rate. The 974 keV line corresponds to a crossover transition

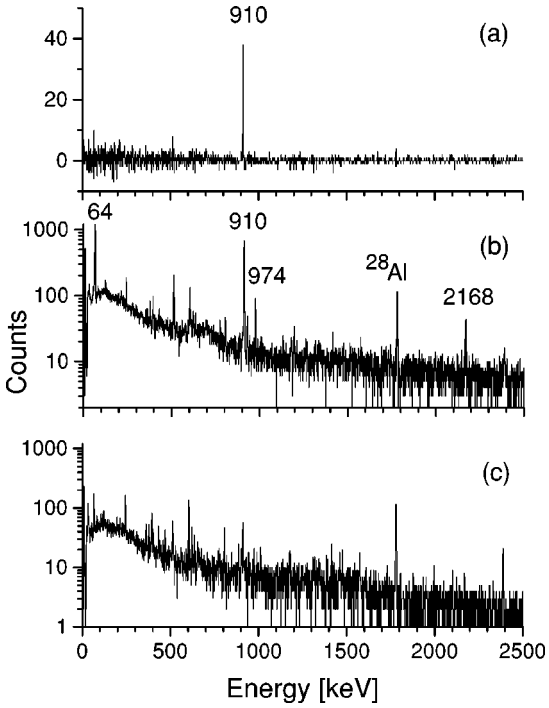

FIG. 5. Partial γ spectra taken in coincidence with β particles at $A=35$. In the upper part (a), the γ spectrum in coincidence with β detection gated by the 64 keV line. In (b) and (c), the γ spectrum in coincidence with β detection and registered in two time bins: 0–300 and 301–600 ms, respectively, after collection. All peaks in spectrum (c) have been identified and belong to daughter activities or long half-life contaminants.

TABLE III. Energy and intensity of γ rays attributed to the ^{35}Al decay.

Energy (keV)	Intensity [a] (relative)	Transition from	Transition to
64.05(30)	100	974	910
124.20(30)	2.5(1.9)	[b]	
910.11(30)	99.7(1.9)	910	0
929.12(40)	5.8(1.3)	[b]	
973.78(20)	11.8(2.4)	974	0
1130.28(40)	3.2(0.9)	[c]	
1194.20(40)	5.3(1.2)	2168	974
2168.24(60)	15.2(3.1)	2168	0
3326.96(70)	18.0(3.6)	[b]	
5629(3)	2.4(1.2)	[c]	

[a]Intensities are relative to the 64 keV γ ray. The intensity per 100 β decays is obtained by multiplying by a factor of 0.45.
[b]Corresponding to transitions in the ^{34}Si level scheme following neutron emission.
[c]Unplaced in the decay scheme.

of the cascade 64–910 keV and the 2168 keV transition is attributed to a branch to the g.s. from a level at this energy. Finally, the energy difference between the 2168 and 974 keV levels corresponds to the third transition, 1194 keV. This line, measured in the $A=35$ experiment at 1194.2(3) keV, should be distinguished from the line we reported at 1193.3(2) keV in the $A=34$ study (Table I). The transitions assigned to the ^{35}Al decay and their intensity are listed in Table III together with three transitions belonging to the ^{34}Si level scheme following β-delayed neutron emission.

The P_n value for ^{35}Al was obtained by measuring the relative intensities of the ^{34}P and ^{35}P activities, as we know that these isotopes are only present as daughter products of the ^{35}Al decay. The resulting P_n value [41(13)%] is larger than that reported previously by Reeder *et al.* [3] [$P_n=26(4)\%$] but in excellent agreement with the result of Lewitowicz *et al.*, $P_n=40(10)\%$ [33,34]. No evidence was found for any $A=33$ activity and $2n$ emission was thus found negligible (the $2n$ emission energy window is equal to 4.3 MeV).

The energy spectrum of the delayed-neutron emission of ^{35}Al measured by the time of flight over 50.8 cm is given in Fig. 6 together with the ^{29}Na delayed-neutron spectrum taken in the same experiment and used for the detection efficiency check. Despite the small solid angle covered by the neutron detectors in this experiment, two maxima can be observed around 3.0 and 0.98 MeV in the spectrum otherwise dominated by prompt β-γ coincidences. The quantitative evaluation of the absolute intensity of these distributions is imprecise since we have to make an assumption for the fraction of the neutron spectrum located below the threshold. Nevertheless, if we take into account the large fraction of the γ rays consecutive to the neutron emission, the neutron energy spectrum reveals that the range of excited levels involved in this process can approximately be traced up to 9 MeV.

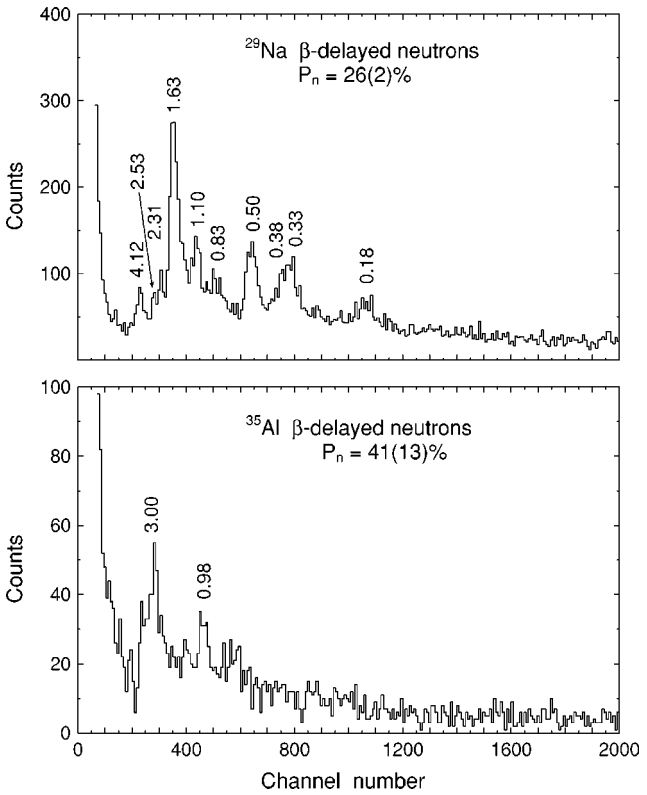

FIG. 6. Neutron time-of-flight spectra taken under identical conditions, with the ^{29}Na sources (upper part) and with the ^{35}Al nuclei (lower part). The time scale is 78 ps/channel. Neutron energies are labeled in MeV.

The β branch to the ^{35}Si ground state has been evaluated by comparing the total γ intensity due to the deexcitation of excited states of ^{35}Si with the decay of ^{35}Si activity and assuming no direct ^{35}Si production. The value deduced from our experiment (3%) is found compatible with the first forbidden character of this transition. Taking into account the new P_n value and the Q_β deduced from Ref. [10], log ft and β-branching values were calculated and reported in Table IV. Also, the conversion coefficient (0.04) of the 64 keV transition can be neglected. The total intensity obtained from Table IV is compatible with the P_n value of 41(13)%.

From systematics in the Al isotopes we have adopted $J^\pi=(5/2)^+$ for the ^{35}Al ($Z=13$, $N=22$) g.s. According to the log ft values, a decay branch from the $J^\pi=(5/2)^+$ g.s. of ^{35}Al to the 974 keV level in ^{35}Si can be considered as an allowed GT decay. From general shell-model considerations, the first positive parity state in the $N=21$ ^{35}Si nucleus results

TABLE IV. β intensities and log ft values in the ^{35}Al β decay to bound levels in ^{35}Si.

E_x (keV)	I_β (%)	log ft	J^π
0	3.0(10)	6.04(14)	$(7/2)^-$
910.10(30)	<0.9	>5.15	$(3/2)^-$
973.80(30)	48(9)	4.70(8)	$(3/2)^+$
2168.10(60)	9.2(19)	5.22(9)	$(5/2)^+$

from a $1p$-$1h$ configuration with a $d_{3/2}$ neutron hole. We propose then, $J^{\pi}=(3/2)^{+}$ for the 974 keV level that will be discussed in more detail in the next section. From previous calculations (see, for example, Refs. [35,36]) and also from systematical trends in neighboring nuclides according to Ref. [10], we take $J^{\pi}=(7/2)^{-}$ for the ^{35}Si g.s. that allows also a good description of the $^{35}\mathrm{Si}\rightarrow{}^{35}\mathrm{P}$ decay, Ref. [36]. We propose $J^{\pi}=(3/2)^{-}$ for the first excited state as expected from the $N=21$ isotone systematics and from the weak β feeding. We have then the sequence $(7/2)^{-}$, $(3/2)^{-}$, $(3/2)^{+}$ for the first three levels corresponding to a cascade with the 64 and 910 keV transitions in an order that has to be determined.

Since the intensities of the 64 and 910 keV energy γ transitions are equal within error limits, their order has to be deduced from level lifetime considerations. As the lowest transition implies a quadrupole character $[(3/2)^{-}\rightarrow(7/2)^{-}]$, an energy of 64 keV would correspond to a lifetime in the microsecond range. Such a lifetime was not observed and therefore the 64 keV transition was placed above the 910 keV transition. This fixes the first excited state at 910 keV. An additional argument for the assignments proposed for the low levels of ^{35}Si is the lifetime of the 974 keV $[J^{\pi}=(3/2)^{+}]$ level. With the energies and multipolarities involved, this lifetime was estimated to be in the range of the delayed-coincidence technique and enables us to test our hypothesis for the multipolarities of the two transitions depopulating this level, namely, $M2$ in competition with a low energy $E1$.

The lifetime of the $J^{\pi}=(3/2)^{+}$ was measured in a separate experiment. The coincidences detected with the thin plastic β counter and the BaF_2 scintillator were registered as two parameter events E_{γ}-t. The time spectrum corresponding to prompt events was determined with a ^{22}Na source. With the ^{35}Al beam, it was found that the 64 keV line as well as the 910 plus 974 lines (not resolved with the BaF_2 counter) gave delayed events in the time spectra. This result revealed the order of the cascade, with the measurable lifetime assigned to the 974 keV level, delaying all consecutive transitions with regard to the β detection. The analysis of the time spectrum was made by selecting events in time and energy ranges as follows. (i) The energy range excluded the lowest part of the spectrum, for which timing properties were found poorly defined; (ii) the time range excluded the portion corresponding to prompt events as defined with the ^{22}Na source. After a determination of the background of the time spectrum in the selected interval, the analysis of the delayed events of the coincidence curve led to the value $\tau=8.5(9)$ ns for the lifetime of the 974 keV level.

In Fig. 7 we have represented the prompt and delayed time spectra and indicated the range of the analysis. The prompt events in the $A=35$ spectrum can be interpreted as events corresponding to large-energy betas firing both detectors. Taking into account the branching ratio [974 keV (11%), 64 keV (89%)], we can express the result for the partial widths in Weisskopf units, which yields $\Gamma/\Gamma_W=0.35(4)\times10^{-3}$ for the 64 keV $E1$ transition and $\Gamma/\Gamma_W=0.061(7)$ for the 974 keV $M2$ transition. These values are typical for similar transitions in light nuclei (see, for example, [37]).

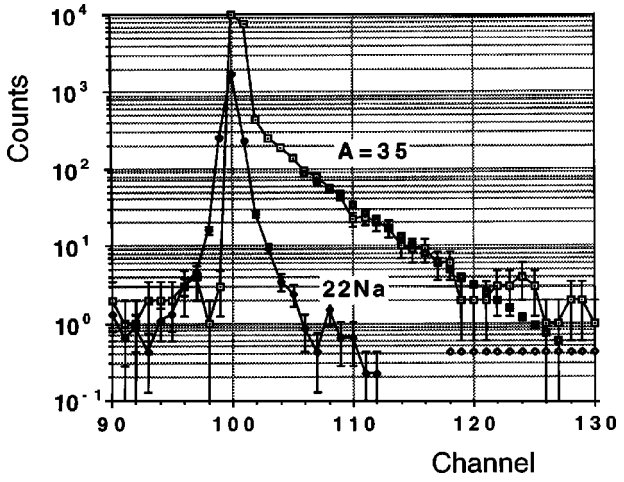

FIG. 7. Delayed coincidences taken in the decay of ^{35}Al with one plastic scintillator recording the β particles and a BaF_2 detector for the γ rays around 900 keV. After background subtraction, the experimental curve was fitted by a single decay (dark squares, ch. 106–127). Time scale: 2.03 ns/channel. ^{22}Na spectrum normalized in area to the $A=35$ delayed component.

We conclude that the different observables obtained in the ^{35}Al decay give supporting evidence for the proposed decay scheme (Fig. 8). β- and γ-transition intensities are in accordance with the proposed J^{π} values of the ^{35}Si levels. Strongly fed in the β decay, the $(3/2)^{+}$ level decays to the ground state by an $M2$ transition in competition with the presumed $E1$ transition $[(3/2)^{+}\rightarrow(3/2)^{-}$, 64 keV]. The

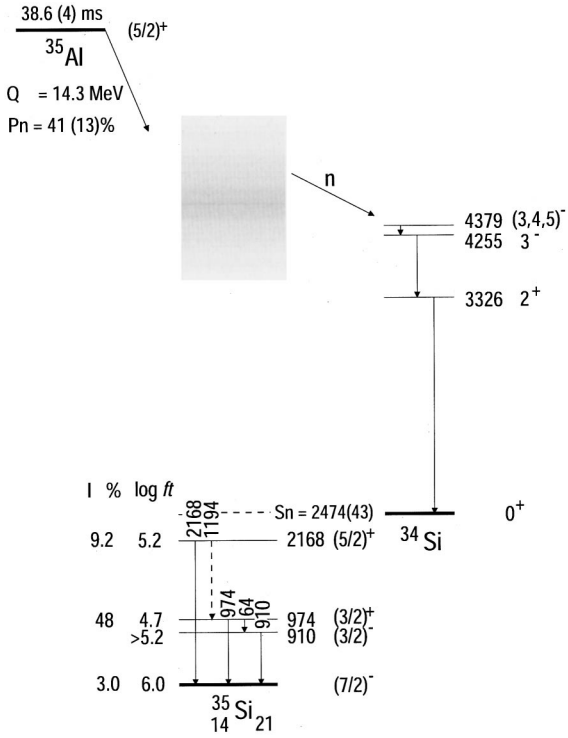

FIG. 8. ^{35}Al β-decay scheme.

relative intensities of these two radiative decays were found to be in good agreement with the typical widths of $M2$ and $E1$ transitions. From the corresponding log ft value, the spin value of the 2168 keV level is limited to $J^{\pi}=(3/2\text{-}7/2)^{+}$. The value $J^{\pi}=(5/2)^{+}$ reported in Fig. 8 resulted from a comparison with the B(GT) calculation given in the next section. The relative intensities of the two decay branches of the $(5/2)^{+}$ level at 2168 keV are compatible with $E1$ and $M1$ radiations for the 2168 and 1194 keV transitions, respectively.

IV. DISCUSSION

A. Derivation of *sd-fp* shell model interaction

In the framework of the shell model we use the sd-fp configuration space for the description of the nuclei under study. It was demonstrated in [20] and then confirmed in [38,39], that protons remain in the sd shell. On the other hand, for neutrons there will be a competititon between $0\hbar\omega$ configurations filling the sd-shell for $N<20$ and the fp-shell for $N>20$ and intruder configurations $1\hbar\omega$ and $2\hbar\omega$ ($sd \rightarrow fp$ excitations).

In a previous work [19], an effective interaction was built for this valence space. It contained three parts: the USD matrix elements [30] from the proton-proton interaction, the KB′ matrix elements [40] for the neutron-neutron interaction and the G matrix of Kahana, Lee, and Scott [41] for the proton-neutron matrix elements. In this mass region, four key nuclei having a simple structure of one particle or one hole in a doubly closed-shell nucleus play a major role for the determination of the interaction: these are ^{39}K, ^{47}K, ^{41}Ca, and ^{35}Si. From the comparison of their spectroscopy with the calculations, strong constraints are provided on some specific monopole parts of the interaction. Between ^{39}K and ^{47}K, the K isotopes can be described to the first order as a one-proton hole in the sd shell and an increasing number of neutrons filling the $f_{7/2}$ orbital. Therefore, from the spectroscopy of ^{39}K–^{47}K we obtain the difference between the $f_{7/2}d_{3/2}$ and $f_{7/2}s_{1/2}$ monopoles. These terms were fixed in our previous work [19] to reproduce the evolution of the $(3/2)^{+}$, $(1/2)^{+}$ doublet along the K isotopes and the position of $(5/2)^{+}$ in ^{47}K. We will leave them unchanged.

As already mentioned at that time, these experimental data are not sufficient to determine all the monopole parameters and the theoretical spectrum of ^{35}Si was (partially arbitrarily) adjusted to the ^{41}Ca one. Again, the $N=21$ isotones from ^{41}Ca to ^{35}Si can be to the first order described by one neutron in the $f_{7/2}$ (or $p_{3/2}$) shell and an increasing number of proton holes in the $s_{1/2}$ and $d_{3/2}$ orbitals (see Fig. 9). Taking into account our ^{35}Si data, we will act only on $p_{3/2}s_{1/2}$ and $p_{3/2}d_{3/2}$ terms to reproduce the evolution of the $(3/2)^{-}$ state. In Table V we give the exact monopole modifications relative to the previous values [19]. The attraction put on the isovector part was balanced with isoscalar repulsion so as to leave ^{41}Ca unmodified. The position of the $(3/2)^{-}$ state in the $N=21$ isotones is shown in Fig. 10 drawn from experiments and calculations. A differential attraction was put on the $p_{3/2}s_{1/2}$ and $p_{3/2}d_{3/2}$ terms to fit the observed kink in the experimental shape of Fig. 10.

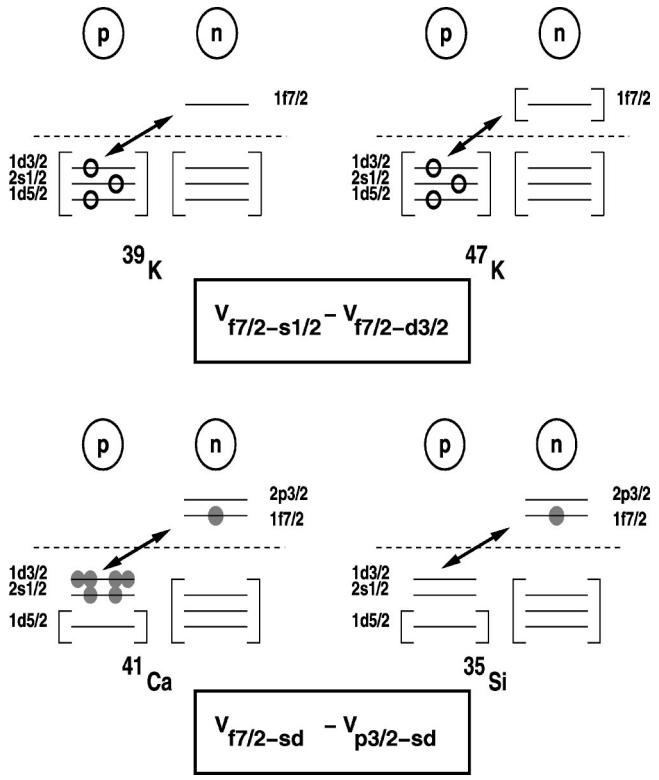

FIG. 9. In the upper part, proton-hole evolution with neutron filling in K isotopes. In the lower part, neutron-particle evolution with the decrease of proton number in $N=21$ isotones.

B. Influence on the physics of *sd-fp* nuclei

The location of the newly observed single-particle states in ^{35}Si can be interpreted as a reduction of the neutron gap between the $f_{7/2}$ and $p_{3/2}$ shells or an erosion of the spin-orbit force far from stability. This erosion is moderate but it is of interest to analyze its consequences, in particular going from the $N=20$ region to the $N=28$ shell gap.

With this intention, a new calculation for $Z<20$, $N>20$ nuclei was made for comparison with our previous estimates [19]. In Table VI we give results for even-even neutron-rich nuclei where comparison with experiment is available. Most of the effect is quite moderate. We report the examples of ^{40}Ar and ^{40}S where the electromagnetic-transition properties remain unchanged. For the $N=28$ isotones, Table VI indicates minor changes again except in the case of ^{42}Si where

TABLE V. Monopole modifications relative to the previous values from Ref. [19] resulting from the determination of the ^{35}Si properties.

	ΔV (MeV)	
	$T=0$	$T=1$
$p_{3/2}s_{1/2}$	+1.35	−0.45
$p_{3/2}d_{3/2}$	+0.21	−0.07

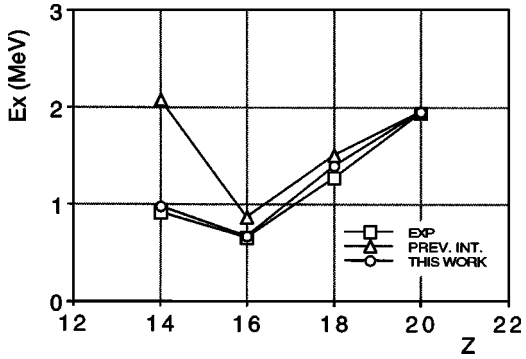

FIG. 10. Evolution of the $(3/2)^-$ excitation energy in $N=21$ isotones. The experimental values (squares) are compared with two calculations using the set of parameters used for the interaction prior to this experiment (triangles), and the single-particle energy for $Z=14$ obtained in this work (circles).

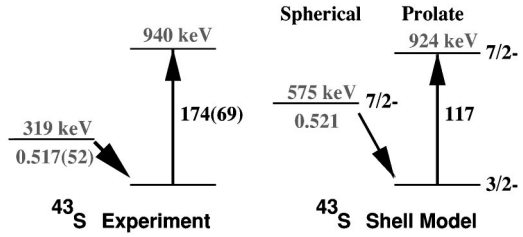

FIG. 11. First excited states in ^{43}S. Shell-model predictions are compared to experimental values (Refs. [4,5]); numbers next to the transitions are $B(E2)$ values in units of e^2 fm^4.

the doubly closed shell character from the study [19] is much less pronounced. This nucleus is very unstable with respect to the choice of the interaction. The reason is that it lies in the transition region between the $N=28$ gap persistence (^{46}Ar,^{44}S) and the vanishing of the shell closure at ^{40}Mg [20].

One aspect not emphasized in [19] is the occurrence of shape coexistence (spherical/prolate) at $N=28$. This has been recently observed and analyzed in the two experiments where the observation of an isomeric state in ^{43}S [5] and the Coulomb excitation measurement of ^{43}S [4] sign the coexistence of spherical and deformed shapes in this nucleus. As explained in Ref. [5], the deformation effect is essentially due to protons, but it is enhanced by the reduction of the $f_{7/2}$-$p_{3/2}$ neutron gap observed in ^{35}Si. Figure 11 presents the observed properties of ^{43}S [4,5] compared with calculations using the interaction deduced from the present study.

C. GT transitions and intruder states in ^{34}Si

The β decay scheme of ^{34}Al resulting from the present work confirms and completes the first study [21]. We have reported β branches to three excited states that are interpreted as negative parity particle-hole states in ^{34}Si.

We have given in Fig. 12 (left part) the theoretical distribution of the Gamow-Teller strength corresponding to three possible values of $J^\pi=(3,4,5)^-$ for the final states in ^{34}Si. The total strength is similar in the three cases, with a broad distribution above the Q_β window peaking around 23 MeV excitation energy. The low-energy part reveals interesting features. Two $J^\pi=3^-$ levels between 4 and 5 MeV are predicted to be populated by strong GT transitions. Comparison with the decay scheme of Fig. 3 shows an excellent agreement for the distribution of the allowed transitions.

A further test of the calculations would be given by the properties of the first two 0^+ and 2^+ states as already discussed in Ref. [20]. This would allow a detailed description of normal and intruder $2p$-$2h$ states. Of these four levels only two (0_1^+ and 2_1^+) are known. A second 2^+ has been tentatively associated with a level at 5.3 MeV [28]. From the present work, two candidates have been found for the $2_1^+ \rightarrow 0_2^+$ transition: either 1193 or 1715 keV. Taking into account Coulomb excitation results [2] and γ-branching estimates, we are led to select the 1193 keV line as the only candidate for a (2_1^+, $E_x=3326$ keV$\rightarrow 0_2^+$) transition in competition with the $2_1^+ \rightarrow 0_1^+$ decay, which can be observed in our spectra with an energy and intensity compatible with recent theoretical calculations. Along this line, we compare the relative intensity of the 1193 and 3326 keV γ rays with the expected value for the $2_1^+ \rightarrow 0_2^+$ and $2_1^+ \rightarrow 0_1^+$ transitions.

If the 3326 and 1193 keV transitions correspond to the two decay branches ($2_1^+ \rightarrow 0_1^+$ and $2_1^+ \rightarrow 0_2^+$) of the 2_1^+ level, we can estimate the $B(E2\uparrow)$ ($0_2^+ \rightarrow 2_1^+$) value using the cor-

TABLE VI. Excitation energies of 2_1^+ (experimental and theoretical) in several nuclei and corresponding $E2$ transitions to the ground state. Values from Ref. [19] are given for comparison.

Nucleus	$E(2^+)$ (MeV)			$B(E2)$ $(2^+\rightarrow 0^+)$ e^2 fm^4		
	Theoretical (this work)	Ref. [19]	Experimental	Theoretical (this work)	Ref. [19]	Experimental
^{40}Ar	1.37	1.37	1.461	43	43	76(3) [a]
^{40}S	0.98	1.05	0.891(13) [b]	77	75	67(7) [b]
^{42}S	1.02	1.07	0.890(15) [b]	94	93	79(12) [b]
^{46}Ar	1.53	1.65	1.554(26) [b]	80	91	39(8) [b]
^{44}S	1.22	1.64	1.297(18) [c]	93	79	63(18) [c]
^{42}Si	1.49	2.56		71	49	

[a]See Ref. [44].
[b]See Ref. [42].
[c]See Ref. [43].

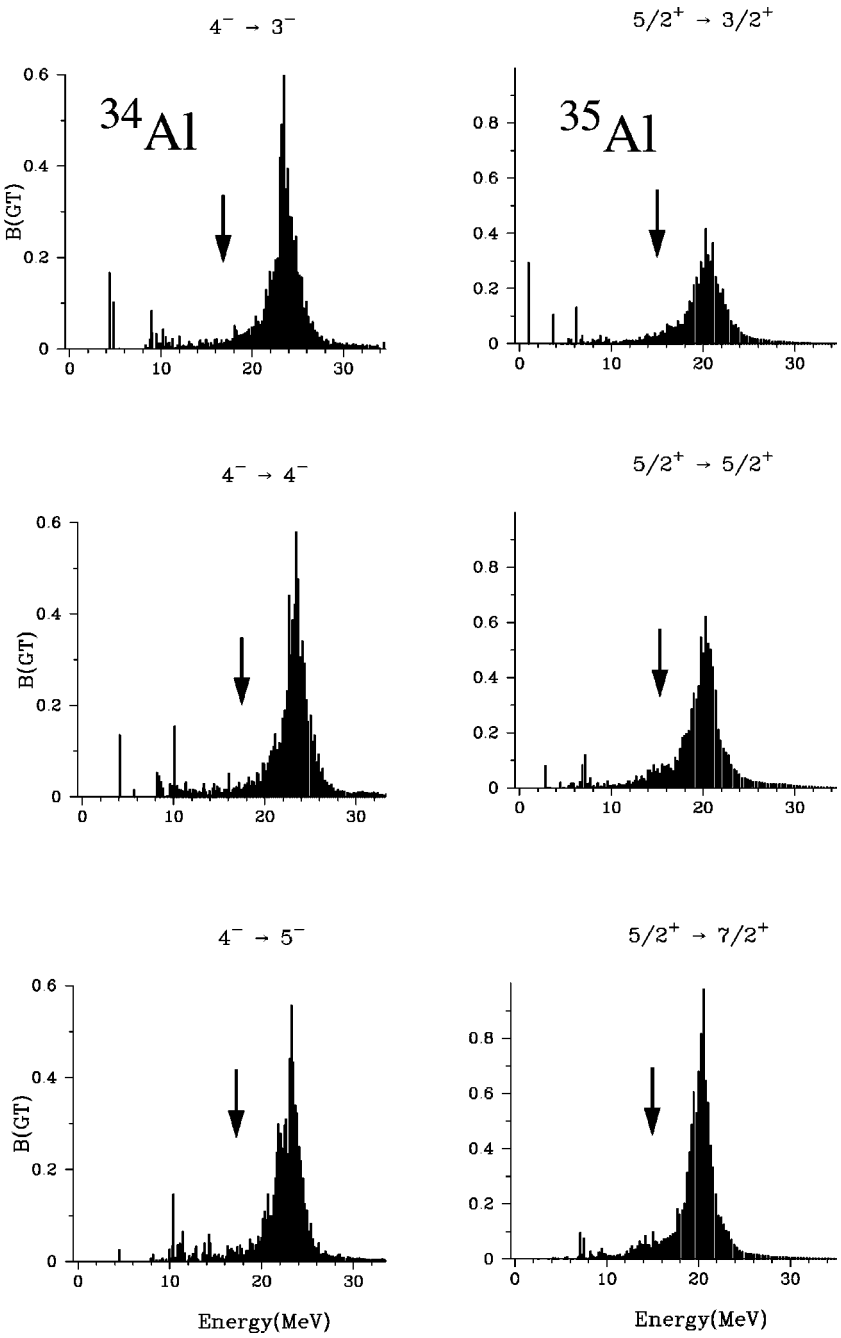

FIG. 12. β decay of ^{34}Al and ^{35}Al. Calculated values of Gamow-Teller strength distribution versus excitation energy in the final nucleus: ^{34}Si on the left and ^{35}Si on the right. The limit of the β-decay window is indicated by the arrow.

rected value of 3.2(6) for the branching ratio (see the Appendix) and the experimental result $[B(E2\uparrow)=85(33)e^2\,\mathrm{fm}^4]$ given previously by Ibbotson *et al.* [2] for the $0_1^+\rightarrow 2_1^+$ transition. After correction by the energy factor, we get $B(E2\uparrow)$ $(0_2^+\rightarrow 2_1^+)=444(210)\ e^2\,\mathrm{fm}^4$. This latter result is consistent with the hypothesis of a $2\hbar\omega$ character for a 0_2^+ state at 2133 keV as well as for the 2_1^+ state.

In Table VII, we have reported energy and $B(E2)$ values calculated for the first three levels of ^{34}Si. For comparison we have indicated experimental results. The overall agreement between the experimental results and those calculated seems satisfying but a further confirmation by a coincidence experiment of the 0_2^+ level is still needed.

How does the 1715 keV transition compare to the 1193 keV transition as a $2_1^+\rightarrow 0_2^+$ candidate? It would imply a 0_2^+ level at 1611 keV. Using the intensity measurement and the $B(E2\uparrow)(0_1^+\rightarrow 2_1^+)$ value as described for the 1193 keV transition, one would get $B(E2\uparrow)$ $(0_2^+\rightarrow 2_1^+)=27(12)\ e^2\,\mathrm{fm}^4$, which is well below the expected value. This result is not consistent with predictions for a $2\hbar\omega$ state, even with mixing assumed.

D. GT transitions in ^{35}Si

The allowed transitions reported in the ^{35}Al decay scheme (Fig. 7) can be compared with the results of the sd-fp shell-model calculations reported in the right part of Fig. 12. In the three GT-strength distributions corresponding to final spin values of $(3/2)^+$, $(5/2)^+$, and $(7/2)^+$, only the low-energy part is relevant for this comparison. A marked feature is that

TABLE VII. ^{34}Si excitation energies (in MeV) and transition probabilities in e^2 fm^4.

J^π	E_x		Transition	$B(E2\uparrow)$	
	Theoretical (this work)	Experimental		Theoretical (this work)	Experimental
0_1^+	0.0	0.0	$0_1^+ \rightarrow 2_1^+$	118	85(33) [a]
0_2^+	2.6	(2.1)	$0_2^+ \rightarrow 2_1^+$	310	444(210) [b]
2_1^+	3.3	3.3	$0_1^+ \rightarrow 2_2^+$	104	<104 [a]
2_2^+	5.4	5.3 [c]			

[a]From Ref. [2].
[b]Indirect estimate, see text.
[c]From Ref. [28].

only two transitions are predicted in the bound range of ^{35}Si levels ($S_n = 2.47$ MeV). The $(3/2)^+$ state is in excellent agreement with the observed 974 keV level. The first $(5/2)^+$ is predicted slightly higher than 2.17 MeV but can clearly be associated with it. Between 6 and 8 MeV excitation energy in ^{35}Si, a complex set of levels given by the calculation allows understanding the main features of the β-delayed neutron spectrum (Fig. 6). Among these, the $(7/2)^+$ levels predicted by the calculation are the best initial-state candidates for transitions to the 2_1^+ final state of ^{34}Si. For these neutrons, an orbital angular momentum transfer $l=4$ is required for the emitted neutron populating the ^{34}Si g.s. and only $l=2$ is required for the 2_1^+ state of ^{34}Si. Therefore most neutron branches are expected to populate the 2_1^+ state.

V. CONCLUSION

A reinvestigation of the neutron-rich ^{34}Al isotope and the next logical step, the study of ^{35}Al, was successful with the 1-GeV pulsed-proton beam on a thick *U* target at CERN. A detailed analysis of the β decays leading to $N=20$ and 21 nuclei, ^{34}Si and ^{35}Si, was made to get a better understanding of the *sd-fp* shell interfaces. The ^{35}Si results have allowed the location of single-particle $p_{3/2}$ and $d_{3/2}$ states, giving an important reference point for extrapolation in shell-model calculations. From comparison of the experimental data with calculated GT distributions, it is concluded that all predicted transitions to bound levels have been observed. Additional information on levels of opposite parity to the β emitting level, revealing the binding energy of the $n\hbar\omega$ excitation, was also obtained.

ACKNOWLEDGMENTS

The authors are grateful to Arthur Pape for a careful reading of the manuscript. This work was supported in part by the European Union Program of Training and Mobility in Research and in part by the IN2P3 (Institut National de Physique Nucléaire et de Physique des Particules). One of the authors (S.N.) would also like to acknowledge the financial support from the Vilho, Yrjö and Kalle Vaisälä Foundation.

APPENDIX: EXTRACTION OF γ INTENSITY FOR A TRANSITION POPULATING A 0^+ EXCITED STATE

In the following, we describe the procedure adopted in the case of the 1193 keV/3326 keV intensity ratio to extract gamma-branching ratios from the β-γ coincidence data. An excited 0^+ state postulated at 2133 keV will decay predominantly by e^+e^- pair emission with a probability of P_π. We calculate from Wilkinson [45] that $P_\pi/P_e = 49$, P_e being the probability of atomic electron emission. In this case, our β-γ detection device, used for the intensity measurements reported in Table I, can be triggered by any of the two electrons emitted as well as by the first beta particle. If the beta-detection probability for a single event is called *P*, it will amount to $3P(1-P)+P^3$ for the higher multiplicity event corresponding to a pair emission consecutive to a beta transition. In our conditions, we estimate an increase of the detection efficiency by a factor of 2.00(25) for the β-γ event associated with the pair emission. The relative intensity of the 1193 keV transition, reported as 6.4(8) in Table I, should be 3.2(6) if this transition populates the 0_2^+ level. A similar correction can be made in the case of the 1715/3326 ratio. For 1715 keV, we calculate $P_\pi/P_e = 9.5$.

[1] T. Motobayashi *et al.*, Phys. Lett. B **346**, 9 (1995).
[2] R.W. Ibbotson *et al.*, Phys. Rev. Lett. **80**, 2081 (1998).
[3] P.L. Reeder, Y. Kim, W.K. Hensley, H.S. Miley, R.A. Warner, Z.Y. Zhou, D.J. Vieira, J.M. Wouters, and H.L. Siefert, in *Proceedings of the International Conference on Exotic Nuclei and Atomic Masses*, Arles, France, 1995, edited by M. de Saint Simon and O. Sorlin (Editions Frontieres, Gif-sur-Yvette, France, 1995), p. 587.
[4] R.W. Ibbotson, T. Glasmacher, P.F. Mantica, and H. Scheit, Phys. Rev. C **59**, 642 (1999).
[5] F. Sarazin *et al.*, in *Proceedings of the XXXVII International Winter Meeting on Nuclear Physics*, Bormio, 1999, edited by I. Iori and A. Moroni (University of Milan, Milan, 1999); F. Sarazin *et al.*, Phys. Rev. Lett. **84**, 5062 (2000).
[6] C. Thibault, R. Klapisch, C. Rigaud, A.M. Poskanzer, R. Prieels, L. Lessard, and W. Reisdorf, Phys. Rev. C **12**, 644 (1975).
[7] C. Detraz, D. Guillemaud, G. Huber, R. Klapisch, M. Langevin, F. Naulin, C. Thibault, L.C. Carraz, and F. Touchard, Phys. Rev. C **19**, 164 (1979).
[8] D. Guillemaud-Mueller, C. Detraz, M. Langevin, F. Naulin, M. de Saint-Simon, C. Thibault, F. Touchard, and M. Epherre,

Nucl. Phys. **A426**, 37 (1984).
[9] G. Klotz, P. Baumann, M. Bounajma, A. Huck, A. Knipper, G. Walter, G. Marguier, C. Richard-Serre, A. Poves, and J. Retamosa, Phys. Rev. C **47**, 2502 (1993).
[10] G. Audi, O. Bersillon, J. Blachot, and A.H. Wapstra, Nucl. Phys. **A624**, 1 (1997).
[11] X. Campi, H. Flocard, A.K. Kerman, and S. Koonin, Nucl. Phys. **A251**, 193 (1975).
[12] A. Watt, R.P. Singhal, M.H. Storm, and R.R. Whitehead, J. Phys. G **7**, L145 (1981).
[13] B.H. Wildenthal, M.S. Curtin, and B.A. Brown, Phys. Rev. C **28**, 1343 (1983).
[14] A. Poves and J. Retamosa, Phys. Lett. B **184**, 311 (1987); Nucl. Phys. **A571**, 221 (1994).
[15] E.K. Warburton, J.A. Becker, and B.A. Brown, Phys. Rev. C **41**, 1147 (1990).
[16] K. Heyde and J.L. Wood, J. Phys. G **17**, 135 (1991).
[17] N. Fukunishi, T. Otsuka, and T. Sebe, Phys. Lett. B **296**, 279 (1992).
[18] T. Otsuka and N. Fukunishi, Phys. Rep. **264**, 297 (1996).
[19] J. Retamosa, E. Caurier, F. Nowacki, and A. Poves, Phys. Rev. C **55**, 1266 (1997).
[20] E. Caurier, F. Nowacki, A. Poves, and J. Retamosa, Phys. Rev. C **58**, 2033 (1998).
[21] P. Baumann, A. Huck, G. Klotz, A. Knipper, G. Walter, G. Marguier, H.L. Ravn, C. Richard-Serre, A. Poves, and J. Retamosa, Phys. Lett. B **228**, 458 (1989).
[22] S. Nummela *et al.*, in *Experimental Nuclear Physics in Europe*, edited by B. Rubio, M. Lozano, and W. Gelletly, AIP Conf. Proc. No. 495 (AIP, Melville, NY, 1999), p. 55.
[23] S. Nummela *et al.*, in *Proceedings of the XXXVIII International Winter Meeting on Nuclear Physics*, Bormio, 2000, edited by I. Iori and A. Moroni (University of Milan, Milan, 2000).
[24] P. Baumann, M. Bounajma, F. Didierjean, A. Huck, A. Knipper, M. Ramdhane, G. Walter, G. Marguier, C. Richard-Serre, B.A. Brown, and the ISOLDE Collaboration, Phys. Rev. C **58**, 1970 (1998).
[25] W. Ziegert *et al.*, *Proceedings of the fourth International Conference on Nuclei Far from Stability* (CERN, Geneva, 1981), p. 327.
[26] M. Bounajma, Thesis, Strasbourg University, 1996.
[27] B. Fornal *et al.*, Phys. Rev. C **49**, 2413 (1994).
[28] L.K. Fifield, C.L. Woods, R.A. Bark, P.V. Drumm, and M.A.C. Hotchkis, Nucl. Phys. **A440**, 531 (1985).
[29] W.A. Mayer, W. Henning, R. Holzwarth, H.J. Körner, G. Korschinek, W.U. Mayer, G. Rosner, and H.J. Scheerer, Z. Phys. A **319**, 287 (1984).
[30] B.H. Wildenthal, Prog. Part. Nucl. Phys. **11**, 5 (1984).
[31] D. Bazin *et al.*, in *Nuclei Far from Stability*, edited by I. S. Towner, AIP Conf. Proc. No. 164 (AIP, New York, 1988), p. 722.
[32] E.K. Warburton and J.A. Becker, Phys. Rev. C **37**, 754 (1988).
[33] M. Lewitowicz *et al.*, Nucl. Phys. **A496**, 477 (1989); A.C. Mueller *et al.*, Z. Phys. A **330**, 63 (1988).
[34] P.M. Endt, Nucl. Phys. **A633**, 1 (1998).
[35] C.L. Woods, Nucl. Phys. **A451**, 413 (1986).
[36] E.K. Warburton and J.A. Becker, Phys. Rev. C **35**, 1851 (1987).
[37] P.M. Endt, At. Data Nucl. Data Tables **55**, 17 (1993).
[38] D.J. Dean, M.T. Ressel, M. Hjorth-Jensen, S.E. Koonin, K. Langanke, and A.P. Zuker, Phys. Rev. C **59**, 2474 (1999).
[39] Y. Utsuno, T. Otsuka, T. Mizusaki, and M. Honma, Phys. Rev. C **60**, 054315 (1999).
[40] A. Poves and A. Zuker, Phys. Rep. **70**, 4 (1981).
[41] S. Kahana, H.C. Lee, and C.K. Scott, Phys. Rev. **180**, 956 (1969).
[42] H. Scheit *et al.*, Phys. Rev. Lett. **77**, 3967 (1996).
[43] T. Glasmacher *et al.*, Phys. Lett. B **395**, 163 (1997).
[44] P.M. Endt, At. Data Nucl. Data Tables **23**, 3 (1979).
[45] D.H. Wilkinson, Nucl. Phys. **A133**, 1 (1969); Nucl. Instrum. Methods **82**, 122 (1970).